Available online at www.sciencedirect.com
ScienceDirect
Current Opinion in Neurobiology

Semi-automated reconstruction of neural circuits using electron microscopy

Dmitri B Chklovskii, Shiv Vitaladevuni and Louis K Scheffer

Reconstructing neuronal circuits at the level of synapses is a central problem in neuroscience, and the focus of the nascent field of connectomics. Previously used to reconstruct the *C. elegans* wiring diagram, serial-section transmission electron microscopy (ssTEM) is a proven technique for the task. However, to reconstruct more complex circuits, ssTEM will require the automation of image processing. We review progress in the processing of electron microscopy images and, in particular, a semi-automated reconstruction pipeline deployed at Janelia Farm. *Drosophila* circuits underlying identified behaviors are being reconstructed in the pipeline with the goal of generating a complete *Drosophila* connectome.

Address
Janelia Farm Research Campus, Howard Hughes Medical Institute, 19700 Helix Drive, Ashburn, VA 20147, United States

Corresponding author: Chklovskii, Dmitri B (mitya@janelia.hhmi.org)

Current Opinion in Neurobiology 2010, **20**:1–9

This review comes from a themed issue on
New technologies
Edited by Erin Schuman and Xiaowei Zhuang

0959-4388/$ – see front matter
Published by Elsevier Ltd.

DOI 10.1016/j.conb.2010.08.002

Introduction

As illustrated by genome sequencing, knowing the structure of biological systems proves essential to interpret their function. In neuroscience, reconstructing the full wiring diagram of a nervous system is an important objective that still remains a major challenge. Such reconstruction requires us to solve two tasks: identifying synapses and tracing neurites that connect them to cell bodies. A list of all neurons and synaptic connections between them, a connectome [1], can only be produced when we successfully solve these tasks.

Although many promising approaches have been put forward [2–4,5•,6,7], only serial-section transmission electron microscopy (ssTEM) has so far provided a proof of concept by reconstructing the complete *C. elegans* nervous system [8••,9••]. Additional attempts have been successful for specific neuropiles with favorable features, as in simple visual systems [10,11•,12]. Here, we discuss reconstruction within the framework of ssTEM, even though many of the reconstruction methods developed for ssTEM could be applied to other electron microscopy techniques and vice versa.

Circuit reconstruction using electron microscopy is a multi-stage process, starting with tissue preparation [13•]. Neural tissue is fixed and labeled with heavy metals to emphasize plasma membranes, necessary for neurite tracing, and synaptic organelles such as neurotransmitter vesicles and pre-synaptic and post-synaptic specializations [14], required for synapse identification. Unfortunately, labeling requirements for the two tasks are often in conflict with each other and the protocol must be optimized for each new neuropile. We found high-pressure freezing and freeze-substitution [15,16] useful in retaining round neurite profiles.

To trace all neurites, embedded tissue should be cut into sections thinner than the 20–30 nm diameter of their terminal processes (Takemura SY, unpublished data, 2010). In practice, ultrathin sections for ssTEM imaging are about 40–50 nm thick [17]. Although finer physical sectioning has been done for imaging in reflection mode [18•,19,20•], doing so for imaging in transmission mode requires significant technology development. Thus, using limited tomography to enhance z-resolution computationally [21,22] appears most promising. After cutting, ultrathin sections are collected on thin Pioloform-coated slot grids and imaged using ssTEM at a few-nanometer resolution [17].

Although the above steps are time-consuming and require exceptional skill, the processing of ssTEM images to produce three-dimensional shapes of neurons and identify synapses is the rate-limiting step. For example, reconstructing the *C. elegans* connectome by manual means took more than 10 years. To reconstruct larger nervous systems requires electron microscopy datasets many orders of magnitude larger and automated image processing. Attaining such automation successfully can make a significant impact on neuroscience by reconstructing biologically interesting circuits.

This article reviews recent developments in electron microscopy image processing, the semi-automated reconstruction pipeline deployed at the Janelia Farm (JF) Research Campus of Howard Hughes Medical Institute, and summarizes its results to date. For the sake of concreteness, we assume that a neural circuit of interest is contained in a reconstructed volume with no dimension

Please cite this article in press as: Chklovskii DB, et al. Semi-automated reconstruction of neural circuits using electron microscopy, Curr Opin Neurobiol (2010), doi:10.1016/j.conb.2010.08.002

greater than a hundred microns. Such volumes encompass most neuropiles of the model species, the fruit fly *Drosophila melanogaster* [23], and are being reconstructed in the JF pipeline (Figure 1).

Reconstruction consists of five main tasks: registration, segmentation, linkage, proofreading, and annotation. Registration places the separately acquired electron microscopy images of different sections and different parts from the same section into vertical and horizontal alignment with each other. Segmentation partitions the stack of images into sets of voxels, defining profiles that belong to distinct neurons. Linkage connects adjacent voxels in consecutive sections that belong to the same cell, so reconstructing these down the z-axis. Although the above steps have been sped up significantly through automation, the reconstruction contains errors, which must be corrected manually in the proofreading step. Annotation identifies pre-synaptic and post-synaptic terminals and neuronal classes.

Reconstruction of volumes from electron microscopy images can be done in two ways: either a 3D approach in which the sections are first aligned into a 3D stack and 3D segmentation performed on this stack to directly obtain 3D volumes [24,25••,26,27••,28•]; or a 2D approach in which each section is segmented separately, the sections are aligned in 3D, and then the 2D segments of adjacent sections linked together to obtain 3D neuronal volumes [29••,30•,31,32]. The 3D approach has the advantage of compartmentalizing the registration and segmentation steps, which allows one to use 3D structural properties of membrane surfaces and intracellular organelles to segment consecutive neurite profiles. In particular, contiguity of neuronal processes that are important in neuron function is valuable for 3D segmentation but unused in 2D. However, the 3D approach has several disadvantages for automated ssTEM: anisotropic resolution makes it difficult to apply 3D segmentation methods to the registered dataset, aligning many hundreds of sections using local transformations is difficult, and registration requires interpolation of pixel values so that segmentation is better done on the original non-registered images. The current JF pipeline therefore follows the second approach (Figure 1).

Figure 1

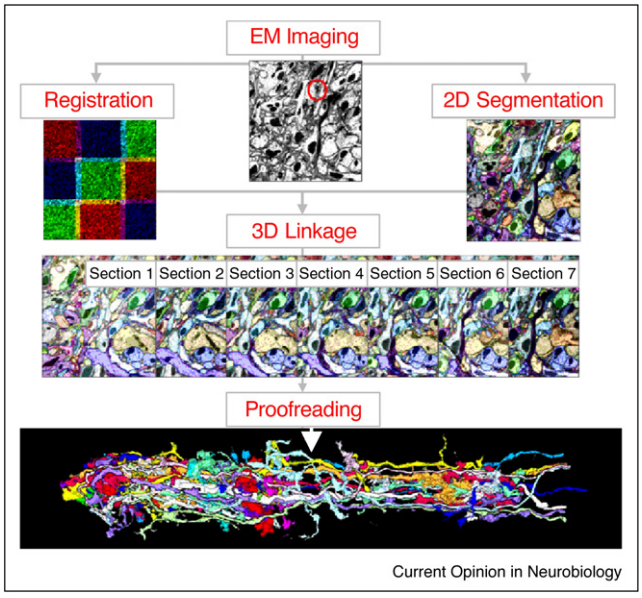

The semi-automated reconstruction pipeline for ssTEM images deployed at Janelia Farm. Automated registration is done in parallel with automated segmentation in 2D. The results of both steps are combined in the automated 3D linkage. Proofreading and annotation are done manually to produce 3D shapes of neurons, synapses and the eventual wiring diagram. The largest dataset being pushed through the pipeline is 90 μm × 90 μm × 80 μm stack from the medulla neuropile of the *Drosophila* optic lobe that includes dozens of columns having a voxel size 3 nm × 3 nm × 40 nm. All synapses (red circle on top panel) can be recognized and most processes of many cells so far reconstructed (one column on bottom panel) can be traced.

Alignment, viewing images, and choosing region of interest

The advantages of computer assistance in image alignment and processing were clear very early on [13•,33], and both public [34,35•,36•] and commercial [37,38] solutions are available. However, the size of recent data sets and more stringent requirements have prompted several groups to attack this problem anew [39,40••,41•,42].

Alignment is conceptually simple but non-trivial in practice, because of imperfections in sectioning and imaging, the high data volume, and the need for completeness [43]. The challenging physical process of sectioning and electron microscopy imaging introduces several complications [13•]. The thin sections of tissue may fold over themselves, and the substrate itself may contain folds. Tissue can tear while being sectioned and the method of high-pressure fixation can create cracks in the sample. Samples shrink as they are imaged, or sections stretch unevenly while they are being cut, leading to scale changes from one micrograph in a mosaic to another. Adjacent sections may be arbitrarily rotated with respect to each other, and so on. Making these problems worse, the procedures cannot select only the best data, or even throw out the worst data, since any significant amount of missing data makes complete reconstruction impossible. The loss of sections during sectioning is particularly damaging to the continuity of reconstruction, yet easily happens when cutting long series.

Alignment typically proceeds in several stages, starting with a rough alignment and creating two outputs — a global and a detailed alignment. The global alignment places all images in a single coordinate system, using simple transforms per image, and is used for proofreading and viewing. The detailed alignment uses more complex

Please cite this article in press as: Chklovskii DB, et al. Semi-automated reconstruction of neural circuits using electron microscopy, Curr Opin Neurobiol (2010), doi:10.1016/j.conb.2010.08.002

and less constrained transformations to better match individual pairs of images, and is used by the automatic tracing software.

The initial rough alignment is usually obtained through an interactive program such as TrakEM2 [40••] or from the imaging coordinates recorded by microscope automation software such as Leginon [44]. If an image contains folds or tears, it is divided into 'patches', each of which is transformed separately. This is necessary since a fold can create mismatches of hundreds or thousands of pixels if a single transform is used for data on both sides of a fold. Most common ssTEM sample problems can be automatically recognized since they are very dark (folds), very light (cracks or tears), or have very low contrast over an extended area (section areas that are thinner or plastic filled vacuoles or cracks filled). After removing these problem areas, the resulting patches have arbitrary shapes.

Next, software uses the rough alignment to compute what patches might overlap, and then uses corresponding features [45] or image correlation [41•] to create more accurate pairwise alignments. This is the most compute intensive step but parallelizes well, allowing the use of thousands of processors.

After obtaining a detailed image transformation between all overlapping image pairs, both in a single section and between consecutive sections, the next step is to fit the transformed images into a global coordinate system used for proofreading and visualization. Correspondence points, derived from the detailed matching, drive a large least squares fit. This is solved using sparse matrix techniques [46] and generates an affine transformation for every patch.

A global solution with a single affine transformation per patch will leave 'seams', or regions that do not exactly match, between the individual images. This does not affect segmentation or linkage, which are done with the more detailed pairwise maps, but it affects the proofreading which is done on the global alignment. The JF pipeline warps the images slightly to make them match at the edges. This compensates both for lens distortion, see also [39], and sample changes during imaging.

Although most electron microscopy image defects can be handled automatically, there are still cases where the current software either cannot identify a problem, or cannot determine the correct fix. (In the lamina and medulla image stacks at JF, the most common such problem is a fold that begins or ends within a section.) These can be fixed manually, but first must be identified and located. An important part of any large-scale alignment system is therefore the reports, plots, and other debugging information needed to allow the user to identify and fix problems.

The result of the alignment process is a set of large images, one per section, typically 30–40K pixels on a side for our data. It is difficult and slow to view even single images of this size in conventional photo-processing software, much less stacks of such images. Since we need not only to view these data, but also to proofread and annotate them, we developed special purpose software, Raveler [47], for this purpose, see Proofreading. Raveler breaks stacks of large images into 'tiles' and loads into memory only those that are necessary. This enables manual operations on the data set (such as selecting a detailed region of interest) with reasonable speed.

2D segmentation

Segmentation is the task of partitioning an image into 'meaningful regions', in this case the electron microscopy images of neural tissue into sets of voxels belonging to distinct neurons. The task is challenging for ssTEM images because membranes are oriented at variable angles relative to the plane of sectioning and as a result present profiles with different appearances, to which are added the problems of differences in labeling and imaging noise, and the presence of intracellular organelles (Figure 2). However, unlike natural images, for which the segmentation problem is ill-posed [48•], for neurite profiles a unique correct answer, in principle, exists.

Segmentation can be used to delineate neuronal profiles either one at a time or all within a region of interest at once. Several methods exist that trace individual profiles relying on user input. In one version [49], the user provides a rough contour outlining the neuron of interest within a section. The active contour algorithm is used to improve the fit to the underlying neuron boundary. A more recent interactive approach to segmentation and visualization of large-scale electron microscopy datasets [50] relies on the active ribbons algorithm [51]. Although active contours and level sets are effective for segmenting single regions, their value seems limited for dense reconstruction in ssTEM because manually seeding many thousands of contours in each section is rather labor intensive. However, it may be possible to use skeleton tracing tools [40••,52•,53•,54] to produce seeds for segmentation.

Complete image segmentation can be divided into two phases: (a) boundary detection, in which a confidence value is computed for each voxel that it lies on a cell boundary, and (b) actual segmentation which partitions voxels based on these boundary confidences.

Generic boundary detection approaches differ in the number of parameters that require a different balance of manual tuning versus machine learning. At one extreme are methods in which only very few parameters must be tuned, such as Canny [55], which convolve a hand-crafted filter

Please cite this article in press as: Chklovskii DB, et al. Semi-automated reconstruction of neural circuits using electron microscopy, Curr Opin Neurobiol (2010), doi:10.1016/j.conb.2010.08.002

Figure 2

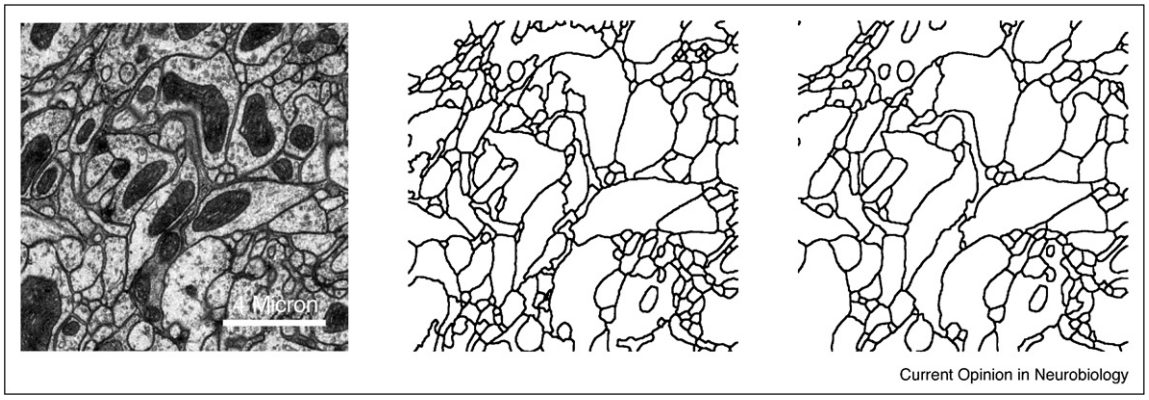

2D segmentation. Left: Original grayscale ssTEM image. Center: Result of automated segmentation. Right: Segmentation ground truth obtained by proofreading automated segmentation.

and pass the results through a manually specified decision function. Next are methods using a large number of manually defined filters, with decision functions involving many parameters, which are trained on the manually labeled, or ground truth, datasets. These methods include pb [48•], non-parametric statistical models [56] and Boosted Edge Learner (BEL) [57•]. Finally, convolutional neural networks [58] learn the filters as well as the parameters of the decision function from the ground truth.

Boundary detection for electron microscopy is both important and challenging and has motivated the development of new segmentation algorithms. These include a Gaussian smoothed Hessian filter at different scales passed through a neural network [30•], Adaboost on intensity and gradient features [59], Radon-like features [60], artificial neural networks [61], convolutional neural net [24,26] and random forests [27••,62•]. The ability to train the detection of boundaries is especially attractive for electron microscopy because the detector can be fine tuned for different preparations, but requires generating ground truth-labeled-datasets for each. Thus, an interactive approach to ground-truth generation implemented recently seems very promising [63••,64••].

The next step is to partition boundary probability maps into distinct neuron profiles, known as multi-way segmentation. A popular choice for generic segmentation [65,66] is to view boundary probability as elevation and apply a watershed algorithm [67,68].

As watershed segmentation is notorious for over-segmentation because of the high density of local minima, this step must be followed by agglomerating these 'superpixels' into neuronal profiles [27••,69]. Agglomerative approaches greedily merge a pair of segments at each iteration until a stopping condition is reached. Although agglomerative segmentation algorithms are greedy, they have the relative advantage of simplicity, smaller space/time complexity and, compared with global optimization [62•], the ease of controlling the tradeoff between false mergers and false splits.

Several criteria have been proposed to arbitrate the mergers, including those based on mean, median and saliency of the boundary between a pair of segments [69–72]. Our experience and quantitative experiments indicate that agglomerative segmentation with mean and median boundary values coupled with BEL boundary detection is highly effective for electron microscopy segmentation [73]. It is also possible to train a machine-learning algorithm to perform agglomeration [27••].

Progress in segmentation requires performance comparison for segmentation algorithms and different parameter settings, which must rely in turn on a framework for quantitative evaluation of the segmentations. There are at least five possibilities:

- Compare segment boundaries of the automatic segmentation against the ground truth by matching individual pixels from the two sets of boundaries. We use the precision-recall measure proposed in the Berkeley Segmentation Dataset [48•] to quantify the fraction of automatic segment boundaries that are correct (precision) and the fraction of ground-truth segment boundaries that are correctly detected (recall) [73]. This algorithm characterizes the accuracy of the boundaries but is not sensitive to minor boundary discrepancies that have major topological implications.
- Compare pixel-pair segment membership using the Rand index [25••,28•,74]. For each pair of pixels, the algorithm determines whether they belong to the same or different segments in the ground truth and automatic

Please cite this article in press as: Chklovskii DB, et al. Semi-automated reconstruction of neural circuits using electron microscopy, Curr Opin Neurobiol (2010), doi:10.1016/j.conb.2010.08.002

segmentation. The Rand index counts the number of pixel-pairs with the same and different attribution in ground truth and automatic segmentation. The advantage of this method is that it avoids solving the correspondence problem between segments from ground truth and automatic segmentation. Yet, it is sensitive to the relative size of the segments.

- Synaptic Rand in which the Rand index is only computed on pre-synaptic and post-synaptic sites. This algorithm may approximate the biological significance of mis-attribution of synapses to different neurons. If synapse annotation is not available then it is also possible to apply a stricter condition by uniformly sampling points along the inside of the boundaries and assuming them to be either pre-synaptic or post-synaptic sites.
- The warping error [75••], which is not sensitive to boundary discrepancies (like the Berkeley benchmark and Rand index), and focuses on topological differences (unlike the Berkeley benchmark). Unlike the Rand index, the magnitude of error reflects the number of boundary locations involved in topological errors, rather than the relative size of the segments.
- Edit distance is used to characterize the amount of work needed to proofread the automatic segmentations. This can be done, for example, by counting the number of splits and mergers needed to convert an automatic segmentation into ground truth. The precise definition depends on the specific proofreading operations used and their cost.

3D linkage

3D linkage identifies pairs of segments in adjacent sections that are likely to belong to the same neuron. There are several techniques that follow a single process from section to section relying either on user input and on-line image processing. In one approach the user-provided contour-trace in one section is propagated to the neuron's outline in the next section, deforming the contour via a Level set energy function [76]. In another approach, the user chooses the neuron of interest in one section and the computer propagates the contour outlining the neuron to the next section using optical flow and Kalman filter techniques [77]. Recently, a two-step estimation-correction procedure has been used to trace processes between sections [50].

Automated dense reconstruction requires linking all processes in a volume without relying on user input. The principal challenges to automated linkage are remaining misalignment between adjacent sections and mistakes in automatic 2D segmentation. To address this challenge, a graph-theoretic approach has been proposed [32], with 2D segments as nodes and directed edges connecting spatially adjacent segments. Neuron volumes are obtained by tracing optimal paths through the stack. Linkage can be formulated as a clustering problem on a graph, with the 2D segments as nodes and edges connecting pairs of segments from adjacent sections likely to belong to the same neuron [30•]. Connected components analysis results in the generation of 3D neuron volumes [29••].

In our framework, a machine learning approach is used to learn the weights of the linkage graph from proofread data. Specifically, each pair of adjacent segments is represented with a feature vector of the intensity statistics in the region of overlap and a boosted classifier is trained to distinguish between link and do not-link pairs. This avoids the need for hand-crafted heuristics and enables fine tuning the linkage for different tissue preparations. To take advantage of multi-neuronal relationships, linkage can be posed as a co-clustering problem which a trainable convex optimization approach has been proposed to solve [78].

The linkage is quantitatively evaluated against ground truth using Rand index and edit distance, which tries to mimic the number of edit operations required of the proofreader to transform the linkage result to ground-truth reconstruction.

Proofreading and annotation

Even state-of-the-art electron microscopy reconstruction techniques are still a long way from computing error-free segmentations of neural tissue [29••]. To provide meaningful connectivity information, it is important to ensure accuracy of the reconstructions and the annotated synapses. We have developed custom software called Raveler to proofread dense reconstructions in large neural volumes with gigapixel cross-section area and 1000+ sections [47] (Figure 3).

Proofreading relies on two kinds of maps produced by the automatic segmentation. First, the 2D segmentation algorithm is run with a very low threshold, thus partitioning the image into superpixels, regions unlikely to belong to two different neurons. Second, the superpixels are grouped into 2D segments. The 2D segments are linked across sections in 3D to generate putative neuron volumes, referred to as 'bodies'. Proofreading is the process of regrouping manually the superpixels, segments and bodies to produce the correct segmentation.

To increase proofreader efficiency, the user is provided with editing tools of varying granularity [47]. At the highest level are 3D-merge, which merges two bodies together, and 3D-split which interactively segments a body into subsets. At the next level, 2D segments can be added to and removed from bodies. On a finer scale, individual superpixels can be added and removed from bodies. Superpixels increase the efficiency of correcting 2D segmentation because in most cases we just need to regroup superpixels — an operation requiring only a few

Please cite this article in press as: Chklovskii DB, et al. Semi-automated reconstruction of neural circuits using electron microscopy, Curr Opin Neurobiol (2010), doi:10.1016/j.conb.2010.08.002

Figure 3

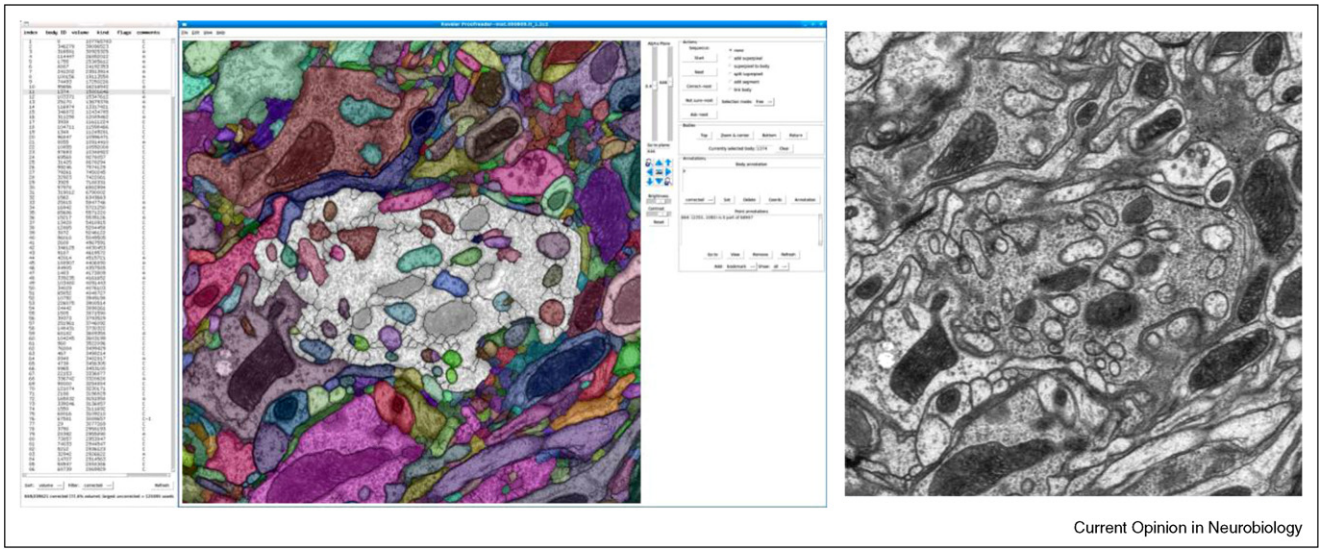

A custom software named Raveler was developed at JF to aid in manual proofreading. Left: The Raveler graphical user interface (GUI) contains a list of bodies, a segmentation image with the highlighted body in white, and the panel with several user operations and information tables. Right: underlying grayscale image that can be toggled in the Raveler GUI.

clicks — rather than painstakingly draw contours dividing up a region, as in manual methods [34]. At the finest level, a superpixel can be split interactively using seeded Graph Cuts [79,80].

After proofreading, the data must be annotated with the location of synapses, indicating the pre-synaptic and post-synaptic sites (in invertebrates such as *Drosophila* and *C. elegans*, it is common for one pre-synaptic site to signal to several post-synaptic sites at a single dyad, triad or tetrad synapse). By combining the synapse annotation with the 3D segmentation, a final wiring diagram is produced.

Results

The JF pipeline has been applied to the lamina and medulla neuropiles of the *Drosophila* optic lobe. The combination of a wide field of view and of high resolution allows both detailed analysis of functional units (cartridges in the lamina, and columns in the medulla) and the interconnections between these modules.

The lamina series is a 6 × 6 mosaic of 2K × 2K images at about 6 nm per pixel (after 2 × 2 binning), 720 sections deep imaged in 22 days. One cartridge has been selected, then aligned, segmented, proofread, and annotated [81]. Since a lamina cartridge has previously been reconstructed manually [11•,82], comparison with this allows us to assess throughput and verify accuracy of the wiring diagram. We find that for neuronal pairs connected by multiple synaptic contacts, the number of contacts in the two wiring diagrams differ by about 10%. In addition, higher resolution and larger extent of the new stack revealed novel connections between known cell types and of one new cell type [81].

The medulla series is a 9 × 9 mosaic of 4K × 4K images, at 3 nm per pixel imaged in 65 days [83]. After overlaps between the images are removed, this volume contains about 250 columns. 1700 sections have been aligned, extending through the medulla, for a volume of 90 μm × 90 μm × 80 μm. Of this, so far a single column has been selected, segmented, proofread and annotated (Figure 1). The six surrounding columns are in progress.

Even with the software in constant and extensive development, automation-assisted reconstruction is already much faster than manual reconstruction [11•,82]. However, the process is still labor intensive. Reconstructing the lamina cartridge took about six person-months and the medulla column about two person-years, some of it dedicated to software testing. These times are dropping as the software is improved, but remain substantial.

Accuracy of the reconstruction is a critical concern and must be monitored at all stages of the pipeline. With the exception of the cases where multiple independent reconstructions of homologous circuits, such as that of the lamina cartridge exist, the error rate in the final wiring diagram is difficult to measure since we lack an independent reconstruction method against which to compare progress. Errors in proofread neuropile segmentations can be identified and quantified by comparing the results

Please cite this article in press as: Chklovskii DB, et al. Semi-automated reconstruction of neural circuits using electron microscopy, Curr Opin Neurobiol (2010), doi:10.1016/j.conb.2010.08.002

from independent proofreaders and different automated segmentation methods. Where this has been done [29••], per thousand 2D profiles we found a few errors that could lead to wiring diagram errors. Expert review left one half to one tenth of these errors unresolved as 'true' ambiguities characterizing the fundamental limit of accuracy of the ssTEM method. These are often traced to adverse causes such as misalignment between consecutive sections, overlapping folds in consecutive sections, and limited z-resolution. The former cause is being addressed by better registration, while the latter two are being addressed by computational super-resolution [21,22].

Finally, both modern genetic methods with reporter lines [84] and older staining methods [85] provide an inventory of neuron types against which morphological comparisons between reconstructed neurons can be made. Where such comparisons have been possible, for example [86], 3D reconstructions from ssTEM closely resemble the forms of known cell types from these light microscopic methods, providing some assurance that ssTEM are accurate. In addition, such matching allows combining information from ssTEM and from cell labeling methods.

Conclusions

Neural circuit reconstruction via stacks of ssTEM images is the only method for which a proof of principle in the form of a complete wiring diagram exists. Although many steps of the reconstruction pipeline have already been automated and improved, further work is necessary and ongoing to speed the reconstruction. As speed increases, so larger biological problems come within reach and untangling all circuits of the entire *Drosophila* nervous system can now be contemplated.

Acknowledgements

We are grateful to I. Meinertzhagen, R. Fetter, P. Winston, J. Nunez-Iglesias, D. J. Olbris, S. Plaza, D. Bock, K. Briggman, A. Cardona, D. Berger, S. Emmons, F. Hamprecht, M. Helmstaedter, V. Jain, V. Kaynig, S. Seung, T. Tasdizen, and S. Turaga for reading the manuscript and for their helpful comments, to I. Meinertzhagen, R. Fetter, K. Harris, P. Rivlin, M. Rivera-Alba, H. Hess and W. Denk for many discussions. We thank Z. Lu, S. Takemura, and R. Fetter for generating ssTEM data and W. Katz for help with Figure 2. We are indebted to all the members of the Janelia Farm Fly EM project for their contributions.

References and recommended reading

Papers of particular interest, published within the period of review, have been highlighted as:

- • of special interest
- •• of outstanding interest

1. Sporns O, Tononi G, Kotter R: **The human connectome: a structural description of the human brain**. *PLoS Comput Biol* 2005, **1**:e42.

2. Lichtman JW, Livet J, Sanes JR: **A technicolour approach to the connectome**. *Nat Rev Neurosci* 2008, **9**:417-422.

3. Helmstaedter M, Briggman KL, Denk W: **3D structural imaging of the brain with photons and electrons**. *Curr Opin Neurobiol* 2008, **18**:633-641.

4. Smith SJ: **Circuit reconstruction tools today**. *Curr Opin Neurobiol* 2007, **17**:601-608.

5. • Denk W, Horstmann H: **Serial block-face scanning electron microscopy to reconstruct three-dimensional tissue nanostructure**. *PLoS Biol* 2004, **2**:e329.
Novel automated electron microscopy technology that signaled the beginning of modern connectomics.

6. Wickersham IR, Lyon DC, Barnard RJ, Mori T, Finke S, Conzelmann KK, Young JA, Callaway EM: **Monosynaptic restriction of transsynaptic tracing from single, genetically targeted neurons**. *Neuron* 2007, **53**:639-647.

7. Livet J, Weissman TA, Kang H, Draft RW, Lu J, Bennis RA, Sanes JR, Lichtman JW: **Transgenic strategies for combinatorial expression of fluorescent proteins in the nervous system**. *Nature* 2007, **450**:56-62.

8. •• White JG, Southgate E, Thomson JN, Brenner S: **The structure of the nervous system of the nematode caenorhabditis elegans**. *Philos Trans R Soc Lond, Ser B, Biol Sci.* 1986, **314**:1-340.
First comprehensive mapping of an entire ivertebrate nervous system.

9. •• Varshney L, Chen B, Paniagua E, Hall D, Chklovskii D: **Stuctural properties of the C. elegans neuronal network**, submitted 2010.
Updated near-complete C. elegans wiring diagram and analysis of its topological properties.

10. Fahrenbach WH: **Anatomical circuitry of lateral inhibition in the eye of the horseshoe crab, Limulus polyphemus**. *Proc R Soc Lond B Biol Sci* 1985, **225**:219-249.

11. • Meinertzhagen IA, Sorra KE: **Synaptic organization in the fly's optic lamina: few cells, many synapses and divergent microcircuits**. *Prog Brain Res* 2001, **131**:53-69.
Wiring diagram of the Drosophila lamina cartridge obtained with ssTEM.

12. Sims SJ, Macagno ER: **Computer reconstruction of all the neurons in the optic ganglion of Daphnia magna**. *J Comp Neurol* 1985, **233**:12-29.

13. • Stevens JK, Davis TL, Friedman N, Sterling P: **A systematic approach to reconstructing microcircuitry by electron microscopy of serial sections**. *Brain Res* 1980, **2**:265-293.
A systematic approach towards vertebrate circuit reconstruction using ssTEM.

14. Kuo J (Ed): *Electron Microscopy: Methods and Protocols*. Humana Press; 2007.

15. Rostaing P, Weimer RM, Jorgensen EM, Triller A, Bessereau JL: **Preservation of immunoreactivity and fine structure of adult C. elegans tissues using high-pressure freezing**. *J Histochem Cytochem* 2004, **52**:1-12.

16. Sosinsky GE, Crum J, Jones YZ, Lanman J, Smarr B, Terada M, Martone ME, Deerinck TJ, Johnson JE, Ellisman MH: **The combination of chemical fixation procedures with high pressure freezing and freeze substitution preserves highly labile tissue ultrastructure for electron tomography applications**. *J Struct Biol* 2008, **161**:359-371.

17. Harris KM, Perry E, Bourne J, Feinberg M, Ostroff L, Hurlburt J: **Uniform serial sectioning for transmission electron microscopy**. *J Neurosci* 2006, **26**:12101-12103.

18. • Knott G, Marchman H, Wall D, Lich B: **Serial section scanning electron microscopy of adult brain tissue using focused ion beam milling**. *J Neurosci* 2008, **28**:2959-2964.
Automated electron microscopy technique with highest isotropic native resolution.

19. Briggman KL, Denk W: **Toward neural circuit reconstruction with volume electron microscopy techniques**. *Curr Opin Neurobiol* 2006, **16**:.

20. • Hayworth KJ, Kasthuri N, Schalek R, Lichtman JW: **Automating the collection of ultrathin serial sections for large volume TEM reconstructions**. *Microscopy and Microanalysis*. 2006:86-87.
Automated serial section technique combining respectable depth resolution and high.

21. Veeraraghavan A, Genkin A, Vitaladevuni S, Scheffer L, Xu S, Hess H, Fetter R, Cantoni M, Knott G, Chklovskii D: **Increasing**

Please cite this article in press as: Chklovskii DB, et al. Semi-automated reconstruction of neural circuits using electron microscopy, Curr Opin Neurobiol (2010), doi:10.1016/j.conb.2010.08.002

depth resolution of electron microscopy of neural circuits using sparse tomographic reconstruction. *CVPR*. 2010.

22. Hu T, et al.: **Super-resolution Reconstruction of Brain Structure Using Sparse Representation over Learned Dictionary**, submitted for publication.

23. Rein K, Zockler M, Mader MT, Grubel C, Heisenberg M: **The Drosophila standard brain**. *Curr Biol* 2002, **12**:227-231.

24. Turaga SC, Murray JF, Jain V, Roth F, Helmstaedter M, Briggman K, Denk W, Seung HS: **Convolutional networks can learn to generate affinity graphs for image segmentation**. *Neural Comput* 2010, **22**:511-538.

25. Turaga SC, Briggman K, Helmstaedter M, Denk W, Seung HS:
•• **Maximin affinity learning of image segmentation**. *NIPS*. 2009.
Proposes a learning algorithm for electron microscopy segmentation that minimizes the Rand index.

26. Jain V, Murray JF, Roth F, Turaga S, Zhigulin V, Briggman KL, Helmstaedter MN, Denk W, Seung HS: **Supervised learning of image restoration with convolutional networks**. *ICCV*. 2007.

27. Andres B, Kothe U, Helmstaedter M, Denk W, Hamprecht F:
•• **Segmentation of SBFSEM volume data of neural tissue by hierarchical classification**. In *Pattern Recognition. 30th DAGM Symposium.* Edited by Rigoll G. Munich, Germany: Springer; 2008:142-152.
Applies random forests classifier on electron microscopy images to generate the membrane probability map and to merge supervoxels into neuronal volumes.

28. Turaga SC, Murray JF, Jain V, Roth F, Helmstaedter M,
• Briggman K, Denk W, Seung HS: **Convolutional networks can learn to generate affinity graphs for image segmentation**. *Neural Comput* 2009.
Applies convolutional neural network and affinity graph to electron microscopy.

29. Mishchenko Y, Hu T, Spacek J, Mendenhall J, Harris K, Chklovskii
•• D: **Ultrastructural analysis of hippocampal neuropil from the connectomics perspective**. *Neuron*, in press.
First dense reconstruction of vertebrate neuropile using ssTEM.

30. Mishchenko Y: **Automation of 3D reconstruction of neural**
• **tissue from large volume of conventional serial section transmission electron micrographs**. *J Neurosci Methods* 2009, **176**:276-289.
Introduces semi-automated reconstruction pipeline for ssTEM.

31. Kaynig V, Fuchs T, Buhmann JM: **Geometrical consistent 3D tracing of neuronal processes in ssTEM data**. *MICCAI*. 2010.

32. Jurrus E, Whitaker R, Jones BW, Marc R, Tasdizen T: **An optimal-path approach for neural circuit reconstruction**. *Proc IEEE Int Symp Biomed Imaging* 2008, **2008**:1609-1612.

33. Macagno ER, Levinthal C, Sobel I: **Three-dimensional computer reconstruction of neurons and neuronal assemblies**. *Annu Rev Biophys Bioeng* 1979, **8**:323-351.

34. Fiala JC: **Reconstruct: a free editor for serial section microscopy**. *J Microsc* 2005, **218**:52-61.

35. ImageJ on World Wide Web URL: http://rsb.info.nih.gov/ij.
•
Comprehensive software for manipulating biological images.

36. Kremer JR, Mastronarde DN, McIntosh JR: **Computer**
• **visualization of three-dimensional image data using IMOD**. *J Struct Biol* 1996, **116**:71-76.
Software for registration and processing electron microscopy images.

37. Glaser JR, Glaser EM: **Neuron imaging with neurolucida — a PC-based system for image combining microscopy**. *Comput Med Imaging Graphics* 1990, **14**:307-317.

38. Stalling D, Westerhoff M, Hege H-C: **Amira: a highly interactive system for visual data analysis**. *The Visualization Handbook*. Elsevier; 2005:. pp. 749–767.

39. Kaynig V, Fischer B, Muller E, Buhmann JM: **Fully automatic stitching and distortion correction of transmission electron microscope images**. *J Struct Biol* 2010, **171**:163-173.

40. Cardona A, Saalfeld S, Preibisch S, Schmid B, Cheng A, Pulokas J,
•• Tomancak P: **An integrated micro- and macroarchitectural analysis of the Drosophila brain by computer-assisted serial section electron microscopy**. *PLoS Biol*, in press.
Integrated software for registration, segmentation, tracing and annotation of electron microscopy images.

41. Anderson JR, Jones BW, Yang JH, Shaw MV, Watt CB,
• Koshevoy P, Spaltenstein J, Jurrus E, Kannan UV, Whitaker RT *et al.*: **A computational framework for ultrastructural mapping of neural circuitry**. *PLoS Biol* 2009, **7**:e1000074.
Introduces a framework for electron microscopy image registration and tracing.

42. Saalfeld S, Cardona A, Hartenstein V, Tomancak P: **As-rigid-as-possible mosaicking and serial section registration of large ssTEM datasets**. *Bioinformatics* 2010, **26**:i57-i63.

43. Kaynig V, Fischer B, Buhmann J: **Probabilistic Image Registration and Anomaly Detection by Nonlinear Warping**, 2008.

44. Suloway C, Pulokas J, Fellmann D, Cheng A, Guerra F, Quispe J, Stagg S, Potter CS, Carragher B: **Automated molecular microscopy: the new Leginon system**. *J Struct Biol* 2005, **151**:41-60.

45. Lowe D: **Object recognition from local scale-invariant features**. *ICCV*. 1999.

46. Li XYS: **An overview of SuperLU: Algorithms, implementation, and user interface Acm Transactions on Mathematical Software**2005, **31(3)**:302-325.

47. Olbris DJ, Winston P, Chklovskii DB: **Raveler — a software for editing large segmented electron microscopy datasets**, in preparation.

48. Martin DR, Fowlkes CC, Malik J: **Learning to detect natural**
• **image boundaries using local brightness, color, and texture cues**.

IEEE Trans Pattern Anal Mach Intell 2004, **26**:530-549.
Comprehensive methodology for machine learning based natural image segmentation and evaluation.

49. Carlbom I, Terzopoulos D, Harris KM: **Computer-assisted registration, segmentation, and 3d reconstruction from images of neuronal tissue-sections**. *IEEE Trans Med Imaging* 1994, **13**:351-362.

50. Jeong WK, Beyer J, Hadwiger M, Vazquez A, Pfister H, Whitaker RT: **Scalable and interactive segmentation and visualization of neural processes in EM datasets**. *IEEE Trans Visual Comput Graphics* 2009, **15**:1505-1514.

51. Reina A, Miller E, Pfister H: **Multiphase geometric couplings for the segmentation of neural processes**. *CVPR*. 2009.

52. Reconstruction software: Program Elegance on World Wide Web
• URL: http://worms.aecom.yu.edu/pages/Reconstruction%20Software.html.
Software for interactive skeleton tracing.

53. Helmstaedter M, Briggman K, Denk W: **KNOSSOS skeleton**
• **tracing tool**, 2010.
Software for interactive skeleton tracing.

54. Helmstaedter M, Briggman KL, Denk W: **High-accuracy neurite tracing for high-throughput neuroanatomy**, in preparation.

55. Canny J: **A computational approach to edge-detection**. *IEEE Trans Pattern Anal Mach Intell* 1986, **8**:679-698.

56. Konishi S, Yuille AL, Coughlan JM, Zhu SC: **Statistical edge detection: learning and evaluating edge cues**. *IEEE Trans Pattern Anal Mach Intell* 2003, **25**:57-74.

57. Dollar P, Tu Z, Belongie S: **Supervised learning of edges and**
• **object boundaries**, 2006.
Boosting algorithm for image segmentation.

58. Lecun Y, Bottou L, Bengio Y, Haffner P: **Gradient-based learning applied to document recognition**. *Proc IEEE* 1998, **86**:2278-2324.

59. Kannan U, Paiva A, Jurrus E, Tasdizen T: **Automatic markup of neural cell membranes using boosted decision stumps**.

Please cite this article in press as: Chklovskii DB, et al. Semi-automated reconstruction of neural circuits using electron microscopy, Curr Opin Neurobiol (2010), doi:10.1016/j.conb.2010.08.002

IEEE Int'l Symp. Biomedical Engineering (ISBI 2009); *Boston, MA: 2009*.

60. Kumar R, Reina A, Pfister H: **Radon-like features and their application to connectomics**. *IEEE Computer Society Workshop on Mathematical Methods in Biomedical Image Analysis (MMBIA)*. 2010.

61. Jurrus E, Paiva AR, Watanabe S, Anderson JR, Jones BW, Whitaker RT, Jorgensen EM, Marc RE, Tasdizen T: **Detection of neuron membranes in electron microscopy images using a serial neural network architecture**. *Med Image Anal* 2010, **14**:770-783.

62. • Kaynig V, Fuchs T, Buhmann J: **Neuron geometry extraction by perceptual grouping in ssTEM images**. *CVPR*. 2010.
Automated segmentation of electron microscopy images using graph cut optimization on random forest classifier.

63. •• On World Wide Web URL: http://ilastik.org.
Software for interactive ground truth generation and automated segmentation for 2D and 3D biological images.

64. •• Trainable Segmentation Plugin (Fiji) on World Wide Web URL: http://pacific.mpi-cbg.de/wiki/index.php/Trainable_Segmentation_Plugin.
Software for interactive ground truth generation and 2D segmentation for ssTEM.

65. Arbelaez P, Maire M, Fowlkes C, Malik J: **From contours to regions: an empirical evaluation**. *CVPR*. 2009.

66. Levner I, Zhang H: **Classification-driven watershed segmentation**. *IEEE Trans Image Process* 2007, **16**:1437-1445.

67. Meyer F: **Un algorithme optimal pour la ligne de partage des eaux**. *Dans 8me congrès de reconnaissance des formes et intelligence artificielle*; *Lyon, France: 1991:847-857*.

68. Vincent L, Soille P: **Watersheds in digital spaces — an efficient algorithm based on immersion simulations**. *IEEE Trans Pattern Anal Mach Intell* 1991, **13**:583-598.

69. Ren X, Malik J: **Learning a classification model for segmentation**. *ICCV*. 2003.

70. Haris K, Efstratiadis SN, Maglaveras N: **Hierarchical image segmentation using contour dynamics**. *ICIP,* 2001.

71. Haris K, Efstratiadis SN, Maglaveras N, Katsaggelos AK: **Hybrid image segmentation using watersheds and fast region merging**. *IEEE Trans Image Process* 1998, **7**:1684-1699.

72. Najman L, Schmitt M: **Geodesic saliency of watershed contours and hierarchical segmentation**. *IEEE Trans Pattern Anal Mach Intell* 1996, **18**:1163-1173.

73. Vitaladevuni S, Mishchenko Y, Genkin A, Chklovskii D: **Segmentation of Neuronal Electron Micrographs**, in preparation.

74. Rand W: **Objective criteria for the evaluation of clustering methods**. *J Am Stat Assoc* 1971, **66**:846-850.

75. •• Jain V, Bollmann B, Richardson M, Berger D, Helmstaedter M, Briggman K, Denk W, Bowden J, Mendenhall J, Abraham W *et al.*: **Boundary learning by optimization with topological constraints**. *CVPR*. 2010.
Proposes a learning algorithm for segmentation of electron microscopy images that minimizes the warping error.

76. Macke JH, Maack N, Gupta R, Denk W, Scholkopf B, Borst A: **Contour-propagation algorithms for semi-automated reconstruction of neural processes**. *J Neurosci Methods* 2008, **167**:349-357.

77. Jurrus E, Hardy M, Tasdizen T, Fletcher PT, Koshevoy P, Chien CB, Denk W, Whitaker R: **Axon tracking in serial block-face scanning electron microscopy**. *Med Image Anal* 2009, **13**:180-188.

78. Vitaladevuni S, Basri R: **Co-clustering of image segments using convex optimization applied to EM neuronal reconstruction**. *CVPR*. 2010.

79. Rother C, Kolmogorov V, Blake A: **"GrabCut" — interactive foreground extraction using iterated graph cuts**. *ACM Trans Graphics* 2004, **23**:309-314.

80. Vu N, Manjunath B: **Graph cut segmentation of neuronal structures from transmission electron micrographs**. *ICIP*. 2008.

81. Rivera-Alba M, de Polavieja G, Lu Z, Chklovskii DB: **Structural features of the Drosophila lamina cartridge**, in preparation.

82. Meinertzhagen IA, O'Neil SD: **Synaptic organization of columnar elements in the lamina of the wild type in Drosophila melanogaster**. *J Comp Neurol* 1991, **305**:232-263.

83. Takemura SY, Meinertzhagen IA, Chklovskii DB: **Wiring of the medulla column in Drosophila**, in preparation.

84. Pfeiffer BD, Jenett A, Hammonds AS, Ngo TT, Misra S, Murphy C, Scully A, Carlson JW, Wan KH, Laverty TR *et al.*: **Tools for neuroanatomy and neurogenetics in Drosophila**. *Proc Natl Acad Sci USA* 2008, **105**:9715-9720.

85. Fischbach KF, Dittrich APM: **The optic lobe of Drosophila melanogaster. 1. A Golgi analysis of wild-type structure**. *Cell Tissue Res* 1989, **258**:441-475.

86. Meinertzhagen IA, Takemura SY, Lu Z, Huang S, Gao S, Ting CY, Lee CH: **From form to function: the ways to know a neuron**. *J Neurogenet* 2009, **23**:68-77.

Please cite this article in press as: Chklovskii DB, et al. Semi-automated reconstruction of neural circuits using electron microscopy, Curr Opin Neurobiol (2010), doi:10.1016/j.conb.2010.08.002